engineering proceedings

Abstract

A Study of Visible-Blind Properties of a SnO_2's Nanowires Network Photodetector †

Estácio P. de Araújo *, Adryelle N. Arantes, Ivani M. Costa and Adenilson J. Chiquito

NanOLaB, Departamento de Física, Universidade Federal de São Carlos, Rodovia Washinton Luiz, Km 235, Monjolinho, São Carlos 13565-905, SP, Brazil; adryelle.fisica@gmail.com (A.N.A.); ivanimcosta@gmail.com (I.M.C.); chiquito@df.ufscar.br (A.J.C.)

* Correspondence: estacio.paiva@gmail.com

† Presented at the 8th International Symposium on Sensor Science, 17–28 May 2021; Available online: https://i3s2021dresden.sciforum.net/.

Keywords: Tin Oxide; nanowire network; visible-blind; MSM photodetector

Summary: We developed an SnO_2 nanowire network visible-blind ultraviolet (UV) photodetector for applications in fields such as safety systems, exposure control, and decontamination processes, among others. Based on the vapor-liquid-solid (VLS) growth method, an SnO_2 nanowire network was synthetized. The sensor was fabricated based on a metal-semiconductor-metal (MSM) structure, and Ag paste was used as a simple and efficient electrical contact. To understand the visible-blind property, two light sources were used: UV (254–365 nm) and VIS (400–900 nm) Lamps. In Current–Voltage measurements, the device under dark and room ambient conditions presented rectifier contacts with different barrier heights; whereas, under UV illumination, the barrier heights seem to be aligned. It was observed that the sensor's photoresponse was optimized for UV Light, with rise and decay times of ~1 s and 3 s, respectively, and exhibited an on/off ratio of 42.5; whereas, for the VIS light, both times were longer, with an on/off ratio of 1.7, both under V = +0.1 V. These results are highly significant for the development of a visible-blind photodetector.

check for updates

Citation: de Araújo, E.P.; Arantes, A.N.; Costa, I.M.; Chiquito, A.J. A Study of Visible-Blind Properties of a SnO_2's Nanowires Network Photodetector. *Eng. Proc.* **2021**, *6*, 40. https://doi.org/10.3390/I3S2021Dresden-10149

Academic Editors: Gianaurelio Cuniberti and Larysa Baraban

Published: 17 May 2021

Publisher's Note: MDPI stays neutral with regard to jurisdictional claims in published maps and institutional affiliations.

Recently, Ultraviolet (UV) light photodetectors have been gaining ground in terms of practice and application, assisting humanity and promoting basic scientific study. Devices that utilize transparent to visible (VIS) light and respond uniquely to UV and deep UV light are certainly useful, e.g., they are commonly employed in solar observation, optical communication, and safety systems such as flame detection [1,2]. Furthermore, the most recent application of these devices can be associated with the quality control of UV light sources employed in biological environments, which can be used in decontamination processes related to the Sars-CoV-2 virus [3,4]. In relation to that, in the future, UV photodetectors will become indispensable devices.

With nanotechnology's development, new possibilities of devices have arisen. The nanometric scale has enabled a better and precise control of physical and chemical parameters, which provides a successful micro and nano electronic market and has given rise to miniaturized devices [5,6]. Semiconductor materials have been demonstrated as excellent candidates to build visible-blind UV photodetectors, such as ZnO [7], TiO_2 [8], GaN [9], SnO_2, among others. Their common property is the large optical gap, which is a basic characteristic demanded for the construction of a UV photodetector. Tin Oxide (SnO_2) is an n-type semiconductor characterized by a wide optical band gap ranging from 3.6 eV to 4.08 eV that belongs to the class of Transparence Conducting Oxides (TCOs). When in its quasi one-dimensional (1D) form, sensors based on SnO_2 have presented a quick detection response, reduced dark current, low operating voltage, and high selectivity, aspects that are indispensable for a reliable photodetector [10]. Besides its applicability as a UV photode-

tector, SnO_2 single nanowire or nanowire network devices have proven to be promising as FET devices [11] and appropriate for gas [12], pH [13], and biologic [14] sensing.

Usually, photodetectors' investigation is focused on the detected wavelength, and little is highlighted regarding their ability to be blind to other frequencies. For instance, the study of nano-structure-based SnO_2 visible-blind photodetectors dates to less than ten years ago, which indicates that there is still a lot to be discussed. In 2015, Ting Xie et al. obtained visible-blind photodetectors based on SnO_2/CuO nano-heterojunctions, in which SnO_2 thin films were deposited by rf-sputtering with CuO nanoparticles placed onto them. A metal-semiconductor-metal (MSM) structure was assembled, and the devices were characterized by a light source of 290 nm, resulting in an on/off ratio of ~592 with a 0.2 V biasing [15]. By 2018, Duo Chen et al. built a visible-blind quasi-solid-state UV detector based on SnO_2-TiO_2 nano-heterostructure arrays. They made a mixture of a polymer and core-shell structure, resulting in an electrolytic solution as the active layer. A Schottky photodetector structure was assembled with a rise time (τ_r) of 0.14 s and a decay time (τ_d) of 0.06 s, under a light source with wavelength and power of 340 nm and 67.4 $\mu W/cm^2$, respectively [16].

In our previous work, using similar SnO_2 nanowire network devices, significant variations of UV photodetector behavior under direct sunlight irradiation were studied. In addition, it was also noted that a sensor's performance depended on the applied electric field [10]. Here we present a study of an SnO_2 nanowire network as a visible-blind photodetector. The nanowire network was grown by the VLS growth technique, and the device was built based on an MSM structure, with two silver paste electrodes. The device was investigated in the dark, under UV wavelength (UV Light), and Visible wavelength (VIS Light) illumination. In the first condition, the current was found to be 8 nA, with V = +0.1 V. Under illumination, the UV Light and VIS Light provided an I_{On}/I_{Off} ratio of 42.5 and 1.7, respectively. The UV Light presented τ_r and τ_d of 1 s and ~3 s, whereas it was 150 s and 200 s for the VIS Light. Our results display a great visible-blind UV photodetector, miniaturized and with high sensitivity and reproducibility.

Tin dioxide nanowires were synthesized based on the vapor-liquid-solid (VLS) growth method [17]. Thin films of gold (15 Å) were deposited (Edwards 306 coating system) in Si/SiO_2 substrates (oxide layer 500 nm thick). The synthesis was carried out in a tube furnace system (Lindberg Blue M), where a high purity Tin powder (0.1 g, Aldrich, purity >99.99%) was placed in an alumina crucible positioned at the center of the furnace and heated to 950 °C for 60 min. For the vapor transport to the synthesis region, an Argon/Oxygen mixture with a constant flow of 20/5 sccm (Mass Flow MKS 1149) was maintained, along with controlled pressure by a vacuum pump around 350 mbar. The as-synthesized products were then examined by scanning electron microscopy (SEM, JEOL JSM 6510, operated at 20 kV), transmission electron microscopy (TEM, FEI Tecnai G2 F20), and X-ray diffraction (XRD, Rigaku D/max-2500, Cu-Kα radiation).

The XDR pattern in Figure 1a depicts the phase composition and synthesis purity. As expected for the tetragonal structure of SnO_2 (a = 4.73 Å e c = 3.18 Å), all diffraction peaks indexed show rutile-like peaks in accordance with JCPDS Card No. 41-1445, and no impurity phases were detected, suggesting a high phase purity of the nanowire network. The general morphological aspects of the products were characterized by scanning electron microscopy (SEM) images, as presented in Figure 1b. We can observe nanowires with rectangular cross-sections and lengths of several micrometers.

Through TEM image and its fast-Fourier transform, the morphology was analyzed and the XRD results previously acquired were ratified as follows. Figure 2a displays a TEM image of a single NW, presenting the desired morphology for this work. A selected region, Figure 2b, shows a HRTEM image indicating that the nanowires are monocrystalline and confirming the sample's high crystalline quality. Figure 2c presents the respective Laue pattern, depicting two sets of planes with spacing of 2.64 Å and 2.36 Å, corresponding to (101) and (200) planes, respectively.

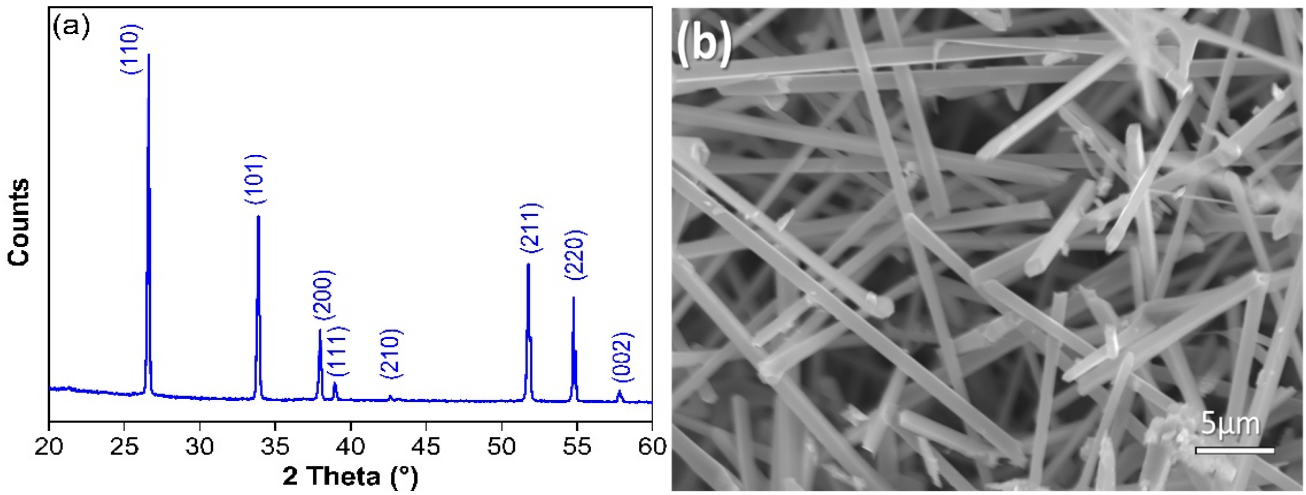

Figure 1. (**a**) XDR pattern of the SnO_2 Nanowire network. All the diffraction peaks were index according to the date rutile tetragonal structure SnO_2 (JCPDS Card No. 41-1445). (**b**) SEM image of the nanowire network.

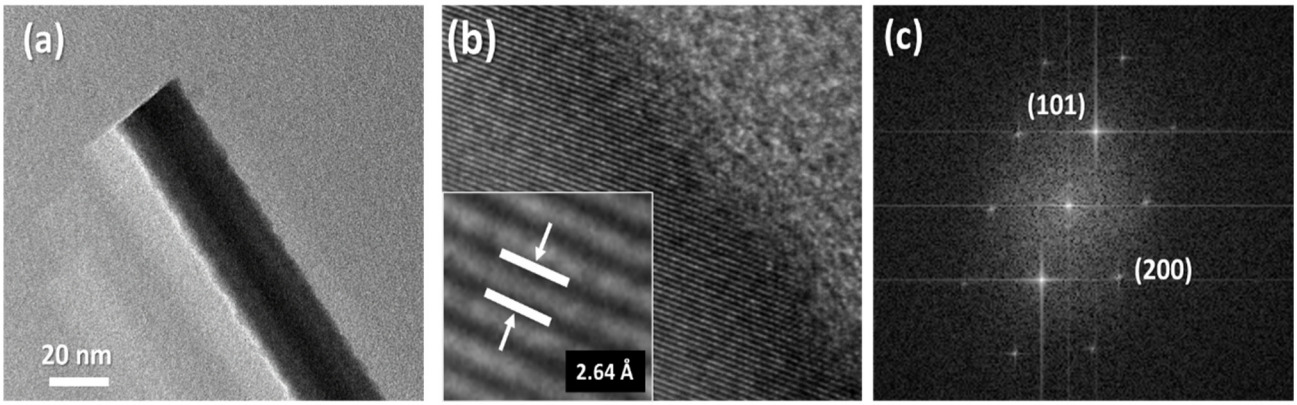

Figure 2. (**a**) TEM image exhibits a SnO_2 NW's. (**b**) HRTEM sets of planes with spacing of 2.64 Å. (**c**) fast-Fourier transform corresponding to (101) and (200) planes of SnO_2's rutile phase.

The devices were manufactured in an MSM structure [10], in which Ag paste was used for the electrical contacts. The fabrication process with Ag paste was chosen due to its high quality mechanical adhesion, not only to the nanowires, because it can penetrate into the nanowire network, inset in Figure 3a, but also to the external electrical circuit, simplifying the assembly of an integrated circuit [18,19]. Before starting a discussion about the visible-blind photodetector and photoconductivity effect in SnO_2 nanowire networks, some details should be discussed. Because a nanowire network contains wires of different sizes and lengths, each one has its own value of surface/volume ratio. In addition, the surface states (broken crystal periodicity) can lead to Fermi pinning on the MS interface, because several different nanowires are in contact with the electrodes, which can modify their transport properties significantly [20]. Therefore, the observed results are the average response of many nanowires being excited. In other words, the electrical response we observe is the randomly percolation pathway chosen by the current to flow from one electrical contact to another, passing through nanowires' homojunctions with different surface/volume ratios [21].

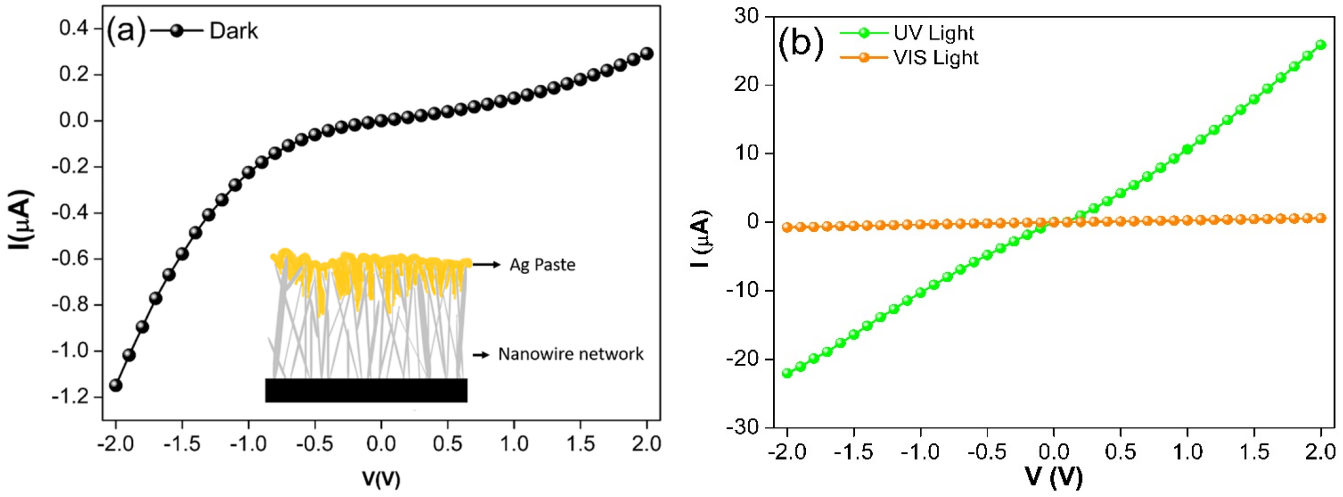

Figure 3. Current-Voltage (I-V) (**a**) curve in dark condition and at room temperature. (**b**) Device under different light sources.

Figure 3a,b, depicts the Current–Voltage (I–V) curves of a nanowire network device with and without illumination, respectively. In Figure 3a, the measurements were performed in the dark and at room ambient conditions; the resistance value was found to be approximately 10^7 Ω. In the Ag/SnO_2 junction, a rectifier behavior arises. Furthermore, one can note that the current for negative biasing is higher than for positive biasing, suggesting the presence of different barrier heights. When under UV illumination, maintaining ambient conditions, a photocurrent effect takes place, modifying the behavior. The sensor is exposed to a UV light source (2 mW/cm^2) with main spectral lines at 254 and 365 nm. Afterwards, it was exposed to a VIS Light (9.5 mW/cm^2), which was coupled to a conventional optical fiber that also acts as an UV filter to avoid any possible contribution from deep blue or even UV wavelengths from the hot filament lamp used. Both sources were positioned 5 cm away from the device. The photocurrent effect can be seen in Figure 3b, with a resistance of approximately 10^5 Ω for the UV Light and 10^7 Ω for the VIS Light.

When analyzing the results from both sources, one can note that the current significantly increases when the device is under UV Light. Firstly, VIS Light's excitation wavelength can generate mostly transition processes from trapping levels to the conduction band (CB), whereas, for the UV Light, the transitions are mainly from the valence band (VB) to the CB. The latter culminates in an electron-hole (e–h) pair formation and, because the electric field force's strength is greater than the Coulombic forces between e-h pairs, they turn into free carriers, improving the conductivity. Figure 3b also displays a linear and symmetrical I–V curve, as would be expected for an ohmic behavior between the nanowire network and the silver paste. However, such results do not confirm the absence of barriers and are better understood when the MSM structure is analyzed by a back-to-back diode model [22]. Furthermore, the UV Light can alter the surface states' population and, consequently, the Fermi level. Owing to the Schottky barrier's dependence on the Fermi level position, the carriers can then perceive and respond to this lower effective barrier height. When it comes to VIS light, the weak photoresponse, i.e., a small current variation, is attributed to sub bands inside the energy gap, which has already been reported for VIS and near infrared excitation of SnO_2 nanowires [23].

Figure 4 shows a sensor's photoresponse. The Current-time (I-t) curves display the behavior of the device under illumination (On) and dark condition (Off). Figure 4a depicts the detector's response to UV Light and VIS Light at a +0.1 V biasing. The On/Off switching was set to 300 s. In the first 300 s, the photodetector is in a dark condition and O_2 molecules are adsorbed on the semiconductor's surface, in which I_{Off}~8 nA was measured. Afterwards, at 300 s, the device is exposed to UV and VIS Light. Under UV Light, the current increases quickly, reaching a plateau region of 0.34 μA; however, this is not observed for the VIS Light, which resulted in I_{on}~15 nA. Therefore, the I_{On}/I_{Off} ratio

calculated for the UV Light and VIS Light are 42.5 and 1.7, respectively. I_{on} is related to the photoexcited e–h pairs' separation by the external electric field; the electrons of SnO_2's VB interact with light and are excited to the CB contributing to the current, whereas holes can move towards the surface, freeing the Oxygen molecules [24]. After the light was turned off, it was observed that the current did not return to its initial value, an effect attributed to recombination processes that were not completely over, mainly due to the trapping of carriers and adsorbed Oxygen molecules.

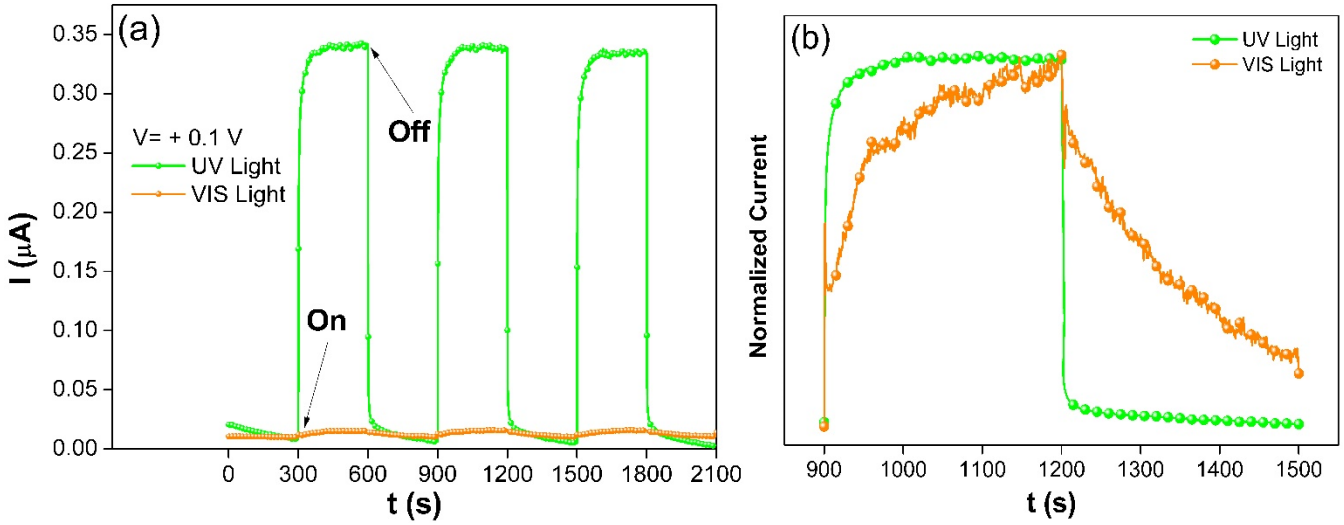

Figure 4. Current-time (I-t) (**a**) Time-dependent photocurrent response of the SnO_2 nanowire network. (**b**) Normalized Current comparison of photocurrent responses.

Figure 4b depicts the normalized time resolved photoresponse of the SnO_2 nanowire network to UV and VIS Light. The τ_r and τ_d were computed; under the UV Light, τ_r ~1 s it was obtained, and for the VIS Light τ_r ~150 s, whereas τ_d was ~3 s and >300 s under the UV Light and VIS Light, respectively. These differences of τ_r and τ_d time between the Lamps can be attributed to band-to-band recombination that restricts the movement of electrons and holes [25]. Furthermore, even though the VIS Light source's power is considerably higher than the UV one, a low response is detected, which then guarantees not only the device's great sensitivity but also its employment/use as a visible-blind photodetector. The values found for photoconductive gain and transient time were compared to values reported for Ga_2O_3, WO_3, and ZnO [26–28]. Our device was proven to be reliable and reproductive, with a photocurrent response great enough for practical applicability and for it to be easily assembled by an uncomplicated fabrication method.

In summary, an SnO_2 nanowire network visible-blind UV photodetector was built based on the VLS growth technique, which generated a nanowire network of excellent quality. The device has an MSM architecture with a simple and easy process of electrode construction. The sensor operated with rise and decay times of 1 s and ~3 s for the UV lamp, while the VIS lamp presented extremely longer times for both. The sensitivity was estimated as 42.5 and 1.7 for the UV and the VIS lamp, respectively. Our results show that the device has a cut-off frequency response, implying that the photodetector responds only to the UV wavelength. Further studies are necessary to fully understand the underlying mechanisms that govern our detectors; the study of the influence of light on the occupation of surface states is necessary. However, the presented results demonstrate that a nanowire network SnO_2 is a promising material for fabricating visible-blind photodetectors.

The authors are thankful for the financial support from the Brazilian agencies: Grant Nos. 2013/19692-0, 2013/07296-2, São Paulo Research Foundation (FAPESP), and Grant Nos. 302640/2010-0 and 305615/2014-9 (CNPq).

Data Availability Statement: The data that support the finding of this study are available from the corresponding author upon reasonable request.

References

1. Tsai, D.-S.; Lien, W.-C.; Lien, D.-H.; Chen, K.-M.; Tsai, M.-L.; Senesky, D.; Yu, Y.-C.; Pisano, A.P.; He, J.-H. Solar-Blind Photodetectors for Harsh Electronics. *Sci. Rep.* **2013**, *3*, 2628. [CrossRef] [PubMed]
2. Omnès, F.; Monroy, E.; Muñoz, E.; Reverchon, J.-L. Wide bandgap UV photodetectors: A short review of devices and applications. *Gallium Nitride Mater. Devices II* **2007**, 64730E. [CrossRef]
3. Goldust, M.; Abdelmaksoud, A.; Navarini, A. Hand disinfection in the combat against COVID-19. *J. Eur. Acad. Dermatol. Venereol.* **2020**, *34*, e454–e455. [CrossRef] [PubMed]
4. Türsen, Ü.; Türsen, B.; Lotti, T. Ultraviolet and COVID-19 pandemic. *J. Cosmet. Dermatol.* **2020**, *19*, 2162–2164. [CrossRef] [PubMed]
5. Chen, H.; Liu, K.; Hu, L.; Al-Ghamdi, A.A.; Fang, X. New concept ultraviolet photodetectors. *Mater. Today* **2015**, *18*, 493–502. [CrossRef]
6. Peng, L.; Hu, L.; Fang, X. Low-Dimensional Nanostructure Ultraviolet Photodetectors. *Adv. Mater.* **2013**, *25*, 5321–5328. [CrossRef]
7. Leung, Y.H.; He, Z.B.; Luo, L.B.; Tsang, C.H.A.; Wong, N.B.; Zhang, W.; Lee, S.T. ZnO nanowires array p-n homojunction and its application as a visible-blind ultraviolet photodetector. *Appl. Phys. Lett.* **2010**, *96*, 053102. [CrossRef]
8. Tsai, T.-Y.; Chang, S.-J.; Weng, W.-Y.; Hsu, C.-L.; Wang, S.-H.; Chiu, C.-J.; Hsueh, T.-J.; Chang, S.-P. A Visible-Blind TiO_2 Nanowire Photodetector. *J. Electrochem. Soc.* **2012**, *159*, J132–J135. [CrossRef]
9. Bugallo, A.D.L.; Tchernycheva, M.; Jacopin, G.; Rigutti, L.; Julien, F.H.; Chou, S.-T.; Lin, Y.-T.; Tseng, P.-H.; Tu, L.-W. Visible-blind photodetector based on p–i–n junction GaN nanowire ensembles. *Nanotechnology* **2010**, *21*, 315201. [CrossRef]
10. de Araújo, E.P.; Arantes, A.N.; Costa, I.M.; Chiquito, A.J. Reliable Tin dioxide based nanowire networks as ultraviolet solar radiation sensors. *Sens. Actuators A Phys.* **2020**, *302*, 111825. [CrossRef]
11. Arantes, A.N.; Araújo, E.P.; Pellegrini, M.; Pedersoli, A.A.; Chiquito, A.J. A simple band model for ultraviolet induced ambipolarity in single SnO_2 nanowire devices. *Phys. E Low-Dimens. Syst. Nanostruct.* **2021**, *128*, 114607. [CrossRef]
12. Ying, Z.; Wan, Q.; Song, Z.T.; Feng, S.L. SnO_2 nanowhiskers and their ethanol sensing characteristics. *Nanotechnology* **2004**, *15*, 1682–1684. [CrossRef]
13. Cheng, Y.; Xiong, P.; Yun, C.S.; Strouse, G.F.; Zheng, J.P.; Yang, R.S.; Wang, Z.L. Mechanism and Optimization of pH Sensing Using SnO_2 Nanobelt Field Effect Transistors. *Nano Lett.* **2008**, *8*, 4179–4184. [CrossRef] [PubMed]
14. Amorim, C.; Blanco, K.; Costa, I.; De Araújo, E.; Arantes, A.; Contiero, J.; Chiquito, A. A New Possibility for Fermentation Monitoring by Electrical Driven Sensing of Ultraviolet Light and Glucose. *Biosensors* **2020**, *10*, 97. [CrossRef] [PubMed]
15. Xie, T.; Hasan, R.; Qiu, B.; Arinze, E.S.; Nguyen, N.V.; Motayed, A.; Thon, S.M.; Debnath, R. High-performing visible-blind photodetectors based on SnO_2/CuO nanoheterojunctions. *Appl. Phys. Lett.* **2015**, *107*, 241108. [CrossRef]
16. Chen, D.; Wei, L.; Meng, L.; Wang, D.; Chen, Y.; Tian, Y.; Yan, S.; Mei, L.; Jiao, J. Visible-blind quasi-solid-state UV detector based on SnO_2 -TiO_2 nanoheterostructure arrays. *J. Alloys Compd.* **2018**, *751*, 56–61. [CrossRef]
17. Costa, I.; Colmenares, Y.; Pizani, P.; Leite, E.; Chiquito, A. Sb doping of VLS synthesized SnO2 nanowires probed by Raman and XPS spectroscopy. *Chem. Phys. Lett.* **2018**, *695*, 125–130. [CrossRef]
18. Hossein-Babaei, F.; Moghadam, S.; Masoumi, S. Forming ohmic Ag/SnO_2 contacts. *Mater. Lett.* **2015**, *141*, 141–144. [CrossRef]
19. Huang, Y.; Lieber, C.M. Integrated nanoscale electronics and optoelectronics: Exploring nanoscale science and technology through semiconductor nanowires. *Pure Appl. Chem.* **2004**, *76*, 2051–2068. [CrossRef]
20. Speckbacher, M.; Treu, J.; Whittles, T.J.; Linhart, W.M.; Xu, X.; Saller, K.; Dhanak, V.R.; Abstreiter, G.; Finley, J.J.; Veal, T.D.; et al. Direct Measurements of Fermi Level Pinning at the Surface of Intrinsically n-Type InGaAs Nanowires. *Nano Lett.* **2016**, *16*, 5135–5142. [CrossRef]
21. Melzi, A.L.R.; Chiquito, A.J. The interplay between Arrhenius and hopping conduction mechanisms in a percolating nanowire network. *J. Phys. D Appl. Phys.* **2016**, *49*, 315303. [CrossRef]
22. Chiquito, A.J.; A Amorim, C.; Berengue, O.M.; Araujo, L.S.; Bernardo, E.P.; Leite, E.R. Back-to-back Schottky diodes: The generalization of the diode theory in analysis and extraction of electrical parameters of nanodevices. *J. Phys. Condens. Matter* **2012**, *24*, 225303. [CrossRef]
23. Shi, H.; Cheng, B.; Cai, Q.; Su, X.; Xiao, Y.; Lei, S. Surface state controlled ultrahigh selectivity and sensitivity for UV photodetectors based on individual SnO_2 nanowires. *J. Mater. Chem. C* **2016**, *4*, 8399–8406. [CrossRef]
24. Costa, I.M.; De Araújo, E.P.; Arantes, A.N.; A Zaghete, M.; Chiquito, A.J. Unusual effects of nanowire-nanowire junctions on the persistent photoconductivity in SnO_2 nanowire network devices. *Nanotechnology* **2021**, *32*, 015702. [CrossRef] [PubMed]
25. Garrido, J.; Monroy, E.; Izpura, I.; Muñoz, E. Photoconductive gain modelling of GaN photodetectors. *Semicond. Sci. Technol.* **1998**, *13*, 563–568. [CrossRef]
26. Zhang, M.; Kang, S.; Wang, L.; Zhang, K.; Wu, Y.; Feng, S.; Lu, W. Facile synthesis of β–Ga_2O_3 nanowires network for solar-blind ultraviolet photodetector. *J. Phys. D Appl. Phys.* **2021**, *54*, 175106. [CrossRef]

27. Huang, K.; Zhang, Q.; Yang, F.; He, D. Ultraviolet photoconductance of a single hexagonal WO_3 nanowire. *Nano Res.* **2010**, *3*, 281–287. [CrossRef]
28. Alsultany, F.H.; Hassan, Z.; Ahmed, N.M. A high-sensitivity, fast-response, rapid-recovery UV photodetector fabricated based on catalyst-free growth of ZnO nanowire networks on glass substrate. *Opt. Mater.* **2016**, *60*, 30–37. [CrossRef]